GRPr Antagonist ^{68}Ga-SB3 PET/CT Imaging of Primary Prostate Cancer in Therapy-Naïve Patients

Ingrid L. Bakker[1], Alida C. Fröberg[1], Martijn B. Busstra[2], J. Fred Verzijlbergen[1], Mark Konijnenberg[1], Geert J.L.H. van Leenders[3], Ivo G. Schoots[1], Erik de Blois[1], Wytske M. van Weerden[2], Simone U. Dalm[1], Theodosia Maina[4], Berthold A. Nock[4], and Marion de Jong[1]

[1]Department of Radiology and Nuclear Medicine, Erasmus MC, Rotterdam, The Netherlands; [2]Deparment of Urology, Erasmus MC, Rotterdam, The Netherlands; [3]Department of Pathology, Erasmus MC, Rotterdam, The Netherlands; and [4]Molecular Radiopharmacy, INRASTES, NCSR "Demokritos," Athens, Greece

The gastrin-releasing peptide receptor (GRPr) is overexpressed in prostate cancer (PCa) cells, making it an excellent tool for targeted imaging. The ^{68}Ga-labeled GRPr antagonist SB3 has shown excellent results in preclinical and clinical studies and was selected for further clinical investigation. The aims of this phase I study were to investigate ^{68}Ga-SB3 PET/CT imaging of primary PCa tumors and assess safety. More aims included an investigation of biodistribution and dosimetry and a comparison with pathology and GRPr expression. **Methods:** Ten therapy-naïve, biopsy-confirmed PCa patients planned for prostatectomy were included. A 3-h extensive PET/CT imaging protocol was performed within 2 wk before prostatectomy. Prostate tissue was evaluated for tumor localization and Gleason score, and in vitro autoradiography was performed to determine GRPr expression. Available MRI scans performed within 3 mo before the study were matched. For dosimetry, residence times were estimated and effective dose to the body as well as absorbed doses to organs were calculated using the IDAC dose model, version 2.1. **Results:** Administration of ^{68}Ga-SB3 (187.4 ± 40.0 MBq, 40 ± 5 μg) was well tolerated; no significant changes in vital signs or laboratory results were observed. ^{68}Ga-SB3 PET/CT showed lesions in 8 of 10 patients. Pathologic analysis revealed a total of 16 tumor lesions, of which PET/CT showed 14, resulting in a sensitivity of 88%. ^{68}Ga-SB3 PET/CT imaging showed uptake in 2 large prostatic intraepithelial neoplasia foci, considered a precursor to PCa, resulting in an 88% specificity. Autoradiography of tumor lesions revealed heterogeneous GRPr expression and was negative in 4 patients. Both PET/CT-negative patients had a GRPr-negative tumor. In autoradiography-positive tumors, the level of GRPr expression showed a significant correlation to tracer uptake on PET/CT. Dosimetry calculations estimated the effective dose to be 0.0144 mSv/MBq, similar to other ^{68}Ga-labeled radiopeptides. The highest absorbed dose was detected in the physiologic GRPr-expressing pancreas (0.198 mGy/MBq), followed by the bladder wall and kidneys. **Conclusion:** ^{68}Ga-SB3 PET/CT is a safe imaging method and a promising tool for early PCa imaging.

Key Words: gastrin-releasing peptide receptor; prostate cancer; tumor imaging; PET/CT

J Nucl Med 2021; 62:1517–1523
DOI: 10.2967/jnumed.120.258814

The gastrin-releasing peptide receptor (GRPr) is a promising tumor target, showing overexpression in multiple cancer types, among which are prostate cancer (PCa), breast cancer, and colon cancer (1).

Physiologic GRPr expression is found throughout the gastrointestinal tract and pancreas (2). Well-differentiated PCa shows higher receptor density than poorly differentiated tumors, and an inverse correlation was found for GRPr expression, Gleason score (GS), and tumor size (3). Also, GRPr expression is present in high-grade prostatic intraepithelial neoplasia (PIN), which is considered a precursor to PCa, with GRPr levels approaching those in PCa (3). Therefore, GRPr-targeting tracers can offer new opportunities for staging and therapy monitoring of PCa.

Multiple GRPr-binding agonists and antagonists have been synthesized for both imaging and therapy purposes (4). We selected the GRPr antagonist SB3 (DOTA-*p*-aminomethylaniline-diglycolic acid-D-Phe-Gln-Trp-Ala-Val-Gly-His-Leu-NHEt) for further clinical investigation after promising preclinical and initial clinical results (5,6). SB3 is chemically based on the previously evaluated ^{99m}Tc-demobesin1 (^{99m}Tc-N_4'-D-Phe6-Gln-Trp-Ala-Val-Gly-His-Leu-NHEt; N4′ = 6-{*p*-[(carboxymethoxy)acetyl]-amino-benzyl}-1,4,8,11-tetraazaundecane), showing high tumor uptake and retention and fast background clearance (7). The ^{99m}Tc-binding N_4' chelator was replaced by a DOTA chelator, enabling theranostic applications.

The primary aims of this phase I clinical study were to investigate the feasibility of imaging primary PCa using ^{68}Ga-SB3 PET/CT and to assess its safety. We tested ^{68}Ga-SB3 imaging by comparing preoperative PET/CT imaging with histopathologic data on the prostatectomy tissue. Other objectives included determining biodistribution, pharmacokinetics, dosimetry, and GRPr expression in tissue samples and comparing with the standard-of-care multiparametric MRI.

MATERIALS AND METHODS

Patients

The study was approved by national and local ethics committees and registered under EudraCT 2011-005859-13. All patients gave written informed consent. Ten newly diagnosed therapy-naïve biopsy-proven PCa patients scheduled for curative prostatectomy were included in the study. If the lower limit of detection was reached, defined by an inability to evaluate visualization of physiologic uptake, the patient was excluded from the study and replaced.

Received Nov. 20, 2020; revision accepted Feb. 16, 2021.
For correspondence or reprints, contact Simone U. Dalm (s.dalm@erasmusmc.nl).
Published online March 31, 2021.

Tracer Synthesis and Radiolabeling

Because SB3 (8) is a non–industry-sponsored compound, the Investigational Medical Product Dossier, Investigational Brochure, and production were approved under local and national supervision. Good-manufacturing-practice–grade SB3 was produced by piCHEM GmbH, and SB3 single-dose kits containing 50 μg of SB3 in 100 μL of 0.01N acetic acid were produced by the good-manufacturing-practice–licensed Erasmus MC Hospital Pharmacy.

SB3 was labeled with ^{68}Ga using Scintomics Robotics; labeling solutions were provided by ABX. The eluate from a ^{68}Ge/^{68}Ga (Eckert and Ziegler) generator was purified, concentrated, and added to a reaction vial together with the SB3 kit dissolved in 3.0 mL of 1.5 M 4-(2-hydroxyethyl)-1-piperazineethanesulfonic acid. The mixture was heated for 10 min at 90°C, allowed to cool for 5 min, purified on a Sep-Pak C_{18} cartridge (Waters), and passed through a sterile 0.2-μm Cathivex GV filter (Merck KGaA).

Safety

Vital functions were registered, and blood samples were collected before, during, and after administration of the radiopharmaceutical. Adverse effects were followed up until surgery.

^{68}Ga-SB3 PET/CT Imaging and Biodistribution

The PET/CT imaging study was performed on a Biograph mCT scanner (Siemens) within 2 wk before surgery. An extensive scan protocol was performed (Fig. 1A; Supplemental Table 1; supplemental materials are available at http://jnm.snmjournals.org). All PET acquisitions were preceded by a low-dose CT scan.

PET images were reconstructed using an ordered-subset expectation maximization algorithm with resolution recovery and time-of-flight information. Quantification of uptake was expressed as SUVs.

To enable optimal imaging of the prostatic region, 40 mg of furosemide were administered at 25 min after injection, and continuous flushing of the bladder was performed.

PET/CT images were independently evaluated by 2 experienced nuclear medicine physicians on an OsiriX 5.9 workstation (Pixmeo Sàrl), and consensus was reported. PET positivity was defined as consistent focal tracer uptake over time in the prostate region and scored as 4 or 5 according to a 5-point Likert score.

Volumes of interest (VOIs) were drawn on ^{68}Ga-SB3 PET/CT fusion images in different volumes depending on the organ of interest. VOIs were positioned by an experienced clinical researcher and checked by a nuclear medicine physician. SUV_{mean} and SUV_{max} in VOIs were measured. Statistical differences in SUV between VOIs were calculated using 2-tailed paired *t* tests.

Histopathologic Analysis

All patients underwent robot-assisted radical prostatectomy, some including extended pelvic lymph node dissection. Tissue was processed according to the standard of care (Fig. 1B; Supplemental Fig. 1). Tumor foci, PIN, and benign prostate hyperplasia were manually delineated by an experienced pathologist. ^{68}Ga-SB3 PET/CT imaging was correlated with pathologic findings by a nuclear medicine physician and pathologist in consensus.

Autoradiography

The GRPr antagonist JMV4168 (DOTA-βAla-βAla-[H-D-Phe-Gln-Trp-Ala-Val-Gly-His-Sta-Leu-NH_2]) was labeled with ^{111}In as previously described (9). Fresh-frozen prostate tissue sections of 10 μm were incubated 1.0 h with 300 μL of 10^{-9} M ^{111}In-JVM416, and blocking studies were performed using either a 1,000-fold excess of Tyr^4-BBN or SB3. Subsequently, phosphor screens were superimposed for 7 d and read on a Cyclone (Perkin Elmer), and tracer binding was quantified as digital light units/mm^2 using OptiQuant software (Perkin Elmer).

Tumor was delineated by a pathologist on adjacent stained tissue slides. The percentage of specific GRPr-positive areas within marked tumor was scored and evaluated by 2 independent readers, and consensus was reported. The level of ^{111}In-JVM4168 binding in tumor areas was quantified and correlated, using the Pearson correlation coefficient, with the SUV_{max} of the corresponding tumor lesion on ^{68}Ga-SB3 PET/CT imaging.

Metabolic Stability and Pharmacokinetics

Blood samples and urine samples were collected at multiple time points (Supplemental Table 2). Radioactivity and degradation of the compound was measured in a γ-counter (1480 Wizard automatic

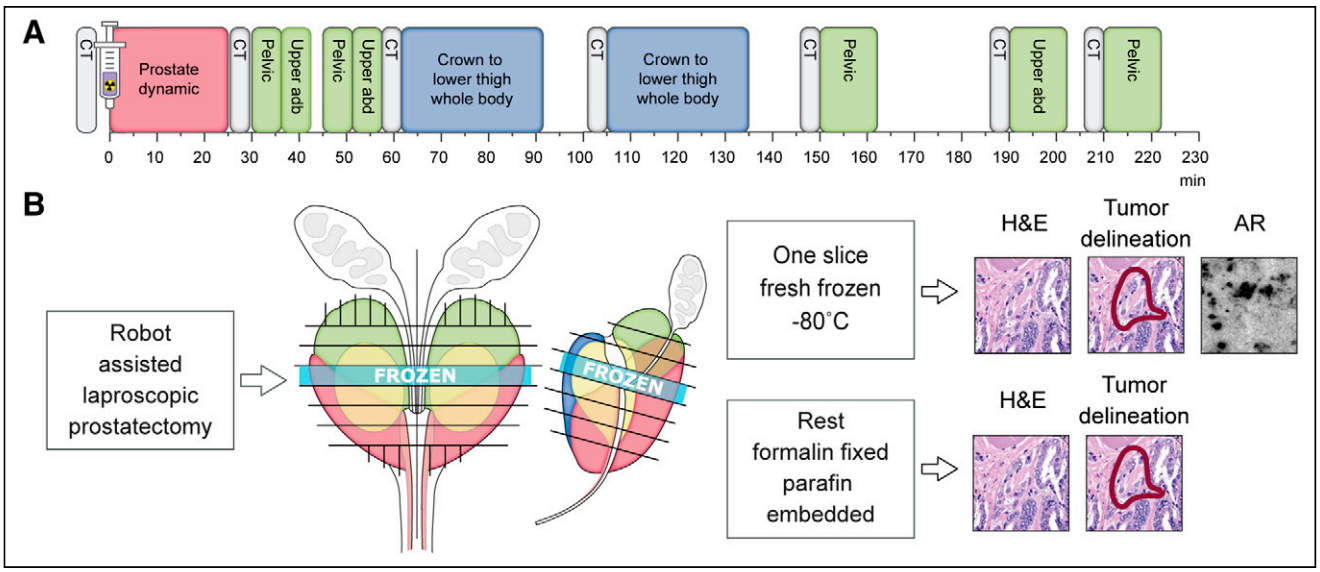

FIGURE 1. Schematic representation of research protocol. (A) Protocol consisting of CT scans (gray), dynamic scan (red), static images (green), and whole-body scans (blue). (B) Tissue was cut into 4-mm sections; 1 section was fresh-frozen, and remainder were formalin-fixed and paraffin-embedded. Slides were stained with hematoxylin and eosin and evaluated by pathologist. Autoradiography was performed on slides of frozen sections. abd = abdomen; AR = autoradiography; H&E = hematoxylin and eosin.

γ-counter; PerkinElmer). Metabolites were registered as previously described (6).

Dosimetry

For organs of interest, time–activity curves were fitted using SUV_{mean} to estimate organ residence times (Prism; GraphPad Software). Goodness of fit was expressed by the R^2 metric, and a minimum R^2 of 0.8 was accepted. Bladder time–activity curves were calculated using the MIRD dynamic bladder model (10) with a 1-h voiding interval. Bone marrow time–activity curves were calculated as previously described (11). Total activity per source organ, absorbed doses, and effective dose were calculated according to International Commission on Radiological Protection publications 103 and 133 and using the IDAC dose model, version 2.1. For dosimetry, residence times were estimated and effective dose to the body, as well as absorbed doses to organs, were calculated using the IDAC dose model, version 2.1.

MRI

The reports of recent MRI scans performed in clinical staging (within 3 mo before study) were selected from the patient files and were therefore masked to the PET/CT and histopathology results of biopsies and radical prostatectomy. The multiparametric MRI protocol was performed as the standard of care after administration of a gadolinium-based contrast agent on a 3.0-T MRI scanner (Discovery MR750; GE Healthcare) using a 32-channel pelvic phased-array coil. The MRI images were reviewed by an experienced urogenital radiologist. Individual lesions were scored according to the guidelines of the Prostate Imaging Reporting and Data System, version 2.

RESULTS

Patients

One patient was excluded and replaced when the lower limit of detection was reached at 1.3 MBq/kg (11 patients were scanned but only 10 patients were included). Five patients also underwent an extended pelvic lymph node dissection.

The average age was 64.1 ± 7.8 y. Prostate-specific antigen levels were 14.3 ± 7.9 μg/L (range, 4–24.8 μg/L) with clinical stages of T1c in 4 patients, T2a in 4 patients, T2c in 1 patient, and T3a in 1 patient. Evaluation of the biopsy cores showed 2 patients with GS 3 + 3 = 6, 6 patients with GS 3 + 4 = 7, 1 patient with GS 4 + 3 = 7, and 1 patient with GS 4 + 4 = 8 (Supplemental Table 3).

Tracer Synthesis and Radiolabeling

All radiolabeling procedures yielded a radiochemical purity of more than 90% and a radiochemical incorporation of more than 99%; the product was sterile and free of bacterial endotoxins.

Safety

Administration proceeded without adverse events. Eight patients experienced discomfort from the flush catheter, including bladder cramps. Catheter position and flush volume were adjusted to relieve symptoms. In 1 patient 1 scan was omitted to allow for adjustments, not reducing the evaluability of the patient.

Full gastrin panels were determined in 8 patients; they showed peak levels 30 min after injection and a steady decline corresponding to normal 60-min postprandial gastrin levels. The peak levels were 100 ± 50 ng/L, comparable to earlier findings of 157.8 ± 67.5 ng/L in healthy persons (12).

^{68}Ga-SB3 PET/CT Imaging and Biodistribution

Patients received 187 ± 40 MBq of ^{68}Ga-SB3 (range, 130–260 MBq; 40 ± 5 μg; 2.2 ± 0.5 MBq/kg). ^{68}Ga-SB3 PET/CT visualized lesions in 8 of 10 patients, 2 examples are shown in Figures 2 and 3. Total-body PET images of all patients can be found in Supplemental Figure 2. In total, 24 potential tumor lesions were identified in the prostate (Table 1). Two patients were suspected of having lymph node metastases.

One unanticipated incidental finding was a spherelike lesion within the cranium. This lesion had an SUV at the level of the blood and was suspected of being a hemangioma (Supplemental Fig. 3). MRI confirmed the diagnosis.

In total, 1,522 VOIs were drawn in 93 scans (Fig. 4; Supplemental Table 4). The average SUV_{max} of suspected tumor lesions was 7.1 ± 4.8 at 60 min after injection (median, 5.5; range, 3.2–22.7). Average tracer uptake in tumor lesions at all time points was 3.3 times higher than that in normal prostate tissue (95% CI, 2.9–3.7). SUV_{mean} showed the same overall distribution as SUV_{max}.

High radioactivity was found in the kidneys (SUV_{max}, 4.1 ± 0.9 at 60 min after injection) and urinary tract. Intense physiologic uptake was observed in the GRPr-expressing pancreas (SUV_{max}, 42.1 ± 15.7 at 60 min after injection). Interestingly, a significantly higher uptake was found in the head of the pancreas than in the tail at all time points, with an average difference of 9.1 SUV_{max} ($P < 0.001$) (at 60 min: head SUV_{max}, 46.3 ± 13.8; tail SUV_{max}, 36.4 ± 16.9). Diffuse uptake was seen throughout the gastrointestinal tract, and more pronounced uptake was seen in the lower esophageal sphincter and the anal sphincter complex. Little physiologic uptake was seen in the thyroid, liver, and spleen ($SUV_{max} < 2$ at 60 min after injection), similar to background tissue.

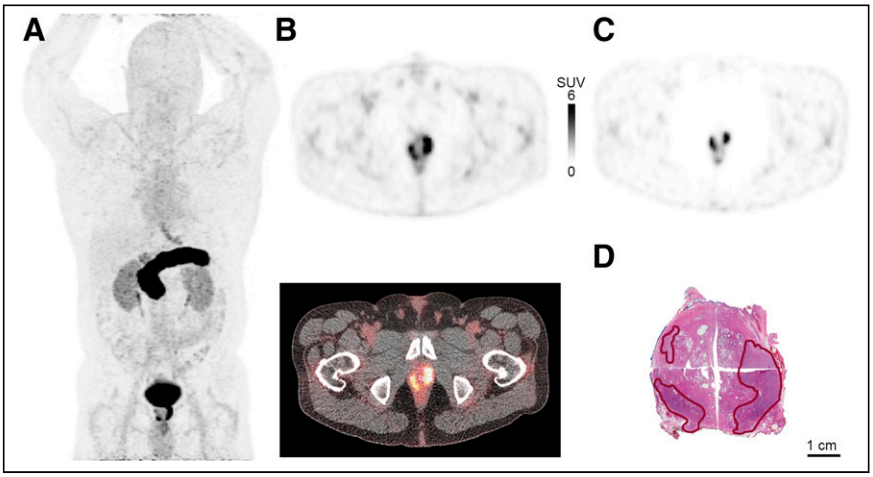

FIGURE 2. ^{68}Ga-SB3 PET/CT imaging of large tumor (GS 3 + 4 = 7) in primary-PCa patient. (A) Maximum-intensity projection 60 min after injection. (B) PET (top) and PET/CT (bottom) imaging 60 min after injection; tumor SUV_{max}, 22.7. (C) PET imaging 210 min after injection; tumor SUV_{max}, 20.0. (E) Corresponding histopathologic slides with tumor delineated in red.

Histopathologic Analysis and Correlation to ^{68}Ga-SB3 PET/CT Imaging

In total, 16 tumor lesions were found in the prostatectomy specimens. In 6

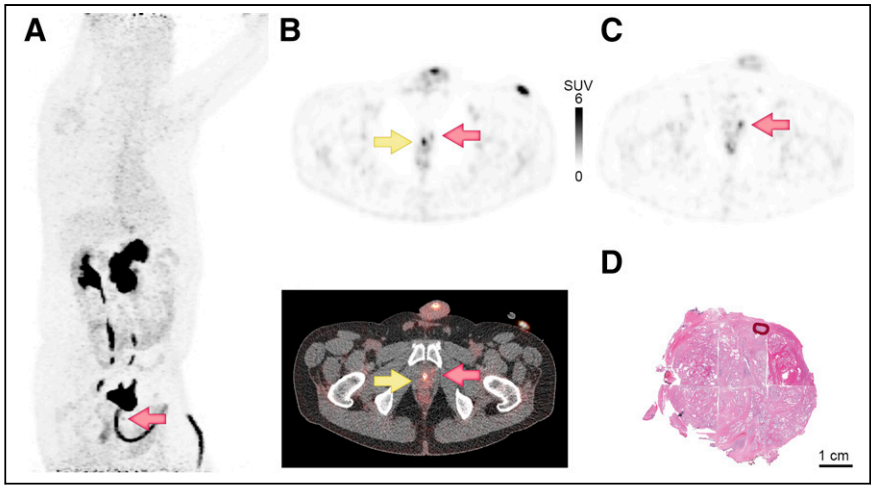

FIGURE 3. ^{68}Ga-SB3 PET/CT imaging of primary PCa patient. Very small tumor (GS 3 + 3 = 6; orange arrows) was not detected in biopsies; however, there was elevated prostate-specific antigen and family history of PCa. Catheter is indicated by yellow arrow. (A) Maximum-intensity projection 60 min after injection. (B) PET (top) and PET/CT (bottom) imaging 60 min after injection; tumor SUV_{max}, 4.4. (C) At 210 min after injection, with catheter removed before scan; tumor SUV_{max}, 4.3. (D) Corresponding histopathologic slides with tumor delineated in red.

patients, 2 separate tumor lesions were identified, with a different GS in 2 patients (Table 1).

Correlation of histopathologic data with ^{68}Ga-SB3 PET/CT imaging revealed 2 false-negative tumors; one was a very small, diffuse-growing GS 3 + 3 = 6 tumor, and the other was a large, solid GS 3 + 4 = 7 tumor. Most PIN lesions were found adjacent to tumor foci and were not separately evaluated. Interestingly, 2 focal hot spots on ^{68}Ga-SB3 PET/CT images were identified as 2 relatively large solitary PIN fields more than 5 mm in diameter (Fig. 5). The sensitivity of ^{68}Ga-SB3 PET/CT for detection of PCa on a lesion basis was 88% (14/16), and specificity was 88% (14/16).

Pathology and ^{68}Ga-SB3 PET/CT revealed lymph node metastases in the same 2 patients; however, lesion-based validation was not achievable.

Autoradiography

Autoradiography with ^{111}In-JVM4168 showed GRPr binding in the tumor foci of all patients, although sometimes only very small tumor foci were observed. Blocking studies confirmed specific uptake (Supplemental Fig. 4). The GRPr expression of tumor was homogeneous in 2 patients and heterogeneous in 4 patients, and autoradiography was negative in 4 patients. Of this last group, 2 patients also had negative ^{68}Ga-SB3 PET/CT findings.

Quantification of GRPr binding in tumor areas was determined and compared with the SUV_{max} of likely corresponding tumor lesions on ^{68}Ga-SB3 PET/CT imaging, showing a significant correlation (Pearson $r^2 = 0.88$ $P < 0.05$) (Supplemental Fig. 5).

Metabolic Stability and Pharmacokinetics

The radiopeptide proved to be very stable in blood (86.4% ± 11.0% at 10 min after injection). It showed little to no degradation in urine (92.1% ± 7.1% at 60 min after injection).

Renal clearance showed a biexponential excretion curve: a fast excretion phase (90%) with a biologic half-life ($t_{1/2}$) of 6 min and the remainder with a $t_{1/2}$ of 242 min. Pancreas and prostate showed monophasic excretions with a $t_{1/2}$ of 180 and 135 min, respectively. An uptake-and-excretion curve was fitted for the tumor with a $t_{1/2}$ of 235 min for the excretion phase (Fig. 6).

Dosimetry

Residence times and absorbed doses are described in Supplemental Table 5. Pancreas showed the highest absorbed dose, 198 μGy/MBq, followed by ureters, bladder wall, and kidneys (134, 116, and 53 μGy/MBq, respectively). Assuming a 1-h voiding model, we estimated an effective dose of 14.4 μSv/MBq, corresponding to 2.66 ± 0.56 mSv in our patients.

MRI

Eight patients had a diagnostic MRI report on file, which revealed 10 tumor foci: 3 that were PI-RADS 3, 3 that were PI-RADS 4, and 4 that were PI-RADS 5. Ten of 13 lesions described on MRI were correlated to ^{68}Ga-SB3 PET/CT, in 8 of 8 patients (Table 1). Only 1 lesion identified by MRI was not detected by PET/CT; this lesion corresponded to a GRPr-negative tumor on autoradiography. Three lesions that were found on PET/CT were not explicitly described by MRI; the data were not adequate to determine whether these were true false-negatives.

DISCUSSION

Currently, multiple radiopharmaceuticals are available for imaging of PCa, predominantly PSMA-targeting compounds, the long-established choline, fluciclovine, and GRPr-targeting compounds (13). PSMA tracers have been proposed to replace choline-based tracers in the current PCa guideline (14). However, limitations for PSMA tracers are still apparent with respect to the sensitivity of early-stage, low-GS tumors (15).

Several GRPr antagonists have been tested in the clinical setting, such as RM2, MJ9, DOTAGA-PEG-RM26, and NeoBOMB1, all coupled to the short-living ^{68}Ga (4,16–18). In a head-to-head comparison in a small patient group, GRPr tumor imaging was comparable to PSMA (19).

With regard to safety, a peptide dose of up to 45 μg of SB3 revealed no serious adverse effects. As expected, the pancreas and urinary tract received the highest absorbed dose, similarly to previously reported ^{68}Ga GRPr antagonists (16,18).

^{68}Ga-SB3 PET/CT visualized tumor foci in 8 of 10 patients. One PET-negative patient had a very small, GS 3 + 3 = 6, diffuse-growing tumor. Considering the average range of ^{68}Ga-produced positrons (1.05 mm in soft tissue), a partial-volume effect is expected in small tumors. However, in a clinical setting it is debatable whether detection of such small tumor foci is relevant. The other PET-negative patient had a large, GS 3 + 4 = 7, solid-growing tumor, which autoradiography conformed to be GRPr-negative. GRPr expression in primary PCa is present in 90%–100% of cases (3,20).

When comparing ^{68}Ga-SB3 with another clinically tested GRPr antagonist, ^{68}Ga-RM2 performance was comparable: SUV_{max} was 7.1 versus 9.1 at 60 min after injection, with sensitivity of 88% versus 85%, respectively (21). We found no clear correlation between

TABLE 1
Tumor Lesion Characteristics

Patient no.	Side of prostate	GS	Autoradiography result	PET score	SUV_{max}	PET result	PI-RADS	MRI result
1	L and R	3 + 4 = 7	++	5	22.7	TP	5	TP
				5	14.4	TP*	5*	TP*
				4	5.9	TP*	5*	TP*
2	L	3 + 4 = 7	+++	5	7.7	TP	4	TP
	R	3 + 3 = 6		5	17.0	TP	—	FN
3	L and R	4 + 3 = 7	+	5	13.3	TP	3	TP
	R	4 + 3 = 7		4	4.7	TP	—	FN
4	L and R	3 + 4 = 7	+	5	9.9	TP	3	TP
				4	6.9	TP*	3*	TP*
5	L	3 + 3 = 6	−	3	5.5	TP	5	TP
	R	4 + 4 = 8		5	5.5	TP	5	TP
				5	6.3	TP*	5*	TP*
				3	3.2	TP*	5*	TP*
				4	5.3	TP*	5*	TP*
6	L	3 + 4 = 7	−	4	5.8	TP	4	TP
	R	3 + 4 = 7		4	5.8	TP	3	TP
	L	PIN		5	4.9	FP		TN
	R	PIN		5	4.8	FP		TN
7	L	4 + 3 = 7	+	4	4.0	TP	5	TP
	R	4 + 3 = 7		5	5.5	TP	—	FN
				5	5.5	TP*	—*	FN*
				4	3.7	TP*	—*	FN*
8	L	3 + 3 = 6	+++	5	4.4	TP	NA	NA
	L	3 + 3 = 6		4	3.6	TP	NA	NA
9	L and R	3 + 4 = 7	−			FN	4	TP
10	L and R	3 + 3 = 6	−			FN	NA	NA

*Grouped results with line above.
− = GRPr-negative; + = 0%–33% GRPr-positive; ++ = 33%–66% GRPr-positive; +++ = 66%–100% GRPr-positive; TP = true positive; FN = false negative; FP = false positive; TN = true negative; NA = not available.

SUV_{max} and GS ($P = 0.11$) or prostate-specific antigen levels ($P = 0.80$), consistent with ^{68}Ga-RM2.

It was reported that in high-grade PIN, considered a precursor to PCa, GRPr expression levels on autoradiography approached those of PCa (3). However, these findings have been challenging to reproduce in a clinical setting. Classification of PIN is difficult, and it is mostly located near or beside tumors. We found 2 relatively large areas of PIN separate from the tumor in 1 patient. Both PIN and PCa were visualized well by ^{68}Ga-SB3. To date, we have found no published data on similar compounds binding to PIN in a clinical setting.

The suspected lymph node metastases on ^{68}Ga-SB3 PET/CT in 2 patients were confirmed by pathology. However, the protocol was not designed to compare lymph node location in histopathology and PET/CT, and with only 2 patients these findings should be considered preliminary.

The diffuse low uptake throughout the gastrointestinal tract may be underestimated because of the partial-volume effect and bowel movement. The higher uptake in the lower esophageal sphincter and anal sphincter complex has been described in GRPr imaging before (5,22) and is most likely caused by the presence of GRPr in smooth muscle cells (23). The uptake pattern was comparable to that of ^{68}Ga-RM2, with comparable pancreatic uptake of around 50 SUV_{max} at 60 min after injection (21).

The administration of furosemide resulted in faster renal clearance but otherwise did not significantly alter tracer uptake in the kidneys.

To our knowledge, this was the first study that showed a significant difference in GRPr uptake between the head and tail of the pancreas. Compared with the head, the corpus and tail have different embryologic origins (24), which may explain differences in cell characteristics. However, the function of GRPr in the pancreas has not yet been described.

The high absorbed pancreatic dose might be a concern for therapy. Gnesin et al. predicted an absorbed pancreatic dose of 1.85 Gy for a theoretic 7.4-GBq ^{177}Lu-labeled MJ9 administration. We published an estimated pancreatic dose of 0.20 mGy/MBq, corresponding to 1.48 Gy for the same administration. This dose can be considered safe when compared with external-beam radiotherapy (18,25).

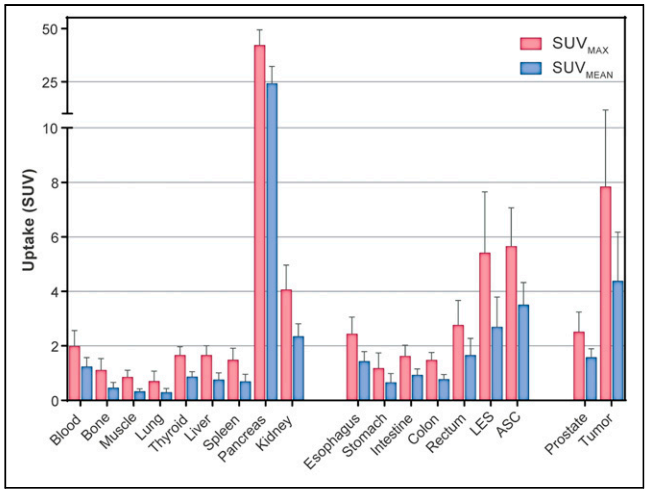

FIGURE 4. Biodistribution of physiologic uptake and tumor uptake of ^{68}Ga-SB3 60 min after injection in therapy-naïve PCa patients. Mean SUV$_{max}$ and SUV$_{mean}$ are depicted with SD. LES = lower esophageal sphincter; ASC = anal sphincter complex.

Low-GS PCa follows the ductal pattern of regular prostate anatomy, which can present as dots in a transaxial slide, and variation in GRPr expression levels per tumor can contribute to heterogeneous expression patterns. In 2 patients, we found good ^{68}Ga-SB3 PET/CT imaging whereas autoradiography showed GRPr negativity, probably because of the small sample size of frozen sections.

Currently, MRI is used for local staging of PCa. ^{68}Ga-SB3 PET/CT performed equally well in local staging of tumor lesions in this small group. However, because of low spatial resolution, PET imaging will not be useful for determining local invasion.

Previous results with ^{68}Ga-SB3 PT/CT imaging in progressive disseminated recurrent PCa patients with a history of antihormonal therapy, which could impact GRPr expression, showed a sensitivity of 55% (5). The excellent stability and tumor-to-background ratios we found, combined with the relatively slower washout of the tumor lesions, is encouraging for the prospect of therapeutic application. ^{177}Lu-SB3 was evaluated in animal studies, where it showed poor in vivo stability. However, this effect could be fully prevented by coinjecting the endopeptidase inhibitor phosphoramidon (26). No clinical data are available yet.

The main limitations of this study were the small number of patients and the varying patient population. Clearly, more clinical studies should be conducted to define the potential theranostic value of this compound.

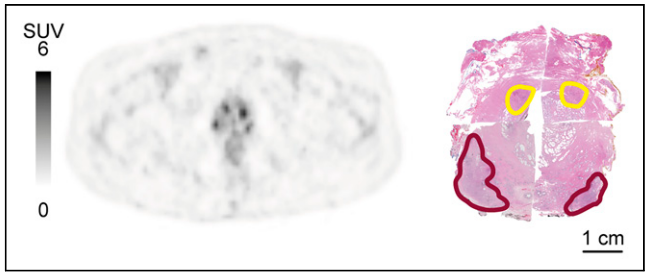

FIGURE 5. Imaging of PCa and high-grade PIN in PCa patient. (Left) SUV PET image 60 min after injection, showing almost equal uptake in PCa and PIN. (Right) Corresponding histopathology slide, with tumor and PIN delineated in red and yellow, respectively.

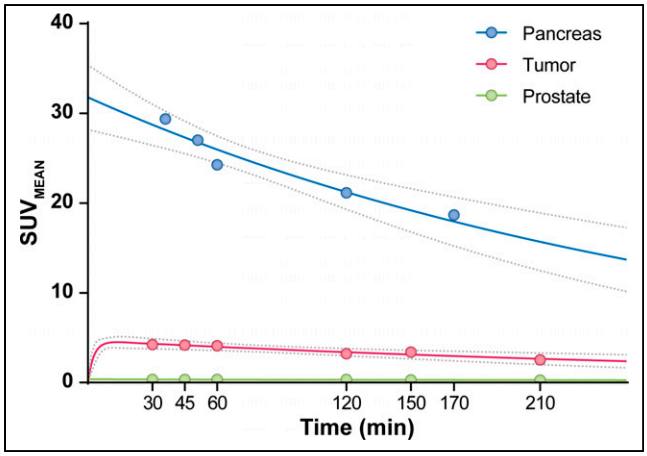

FIGURE 6. Pharmacokinetic excretion patterns of ^{68}Ga-SB3 from pancreas, tumor, and normal prostate. Pancreas and prostate show excretion with biologic half-time of 196 and 135 min, respectively. Excretion phase of tumor shows half-time of 235 min. Fits (solid lines) and 95% CIs (dotted lines) are indicated.

CONCLUSION

The GRPr antagonist ^{68}Ga-SB3 has shown excellent imaging qualities and is safe to use in primary-PCa patients, with high sensitivity for early-stage PCa. ^{68}Ga-SB3 has an attractive biodistribution pattern with fast renal clearance and relatively long tumor retention.

DISCLOSURE

No potential conflict of interest relevant to this article was reported.

ACKNOWLEDGMENTS

We thank all employees of the Department of Radiology and Nuclear Medicine at Erasmus for their collaborative effort to realize this locally sponsored radiolabeled drug research. In particular, we thank Wout Breeman, Paul Janssen, and Margreet van der Meij for aiding in IMPD and IB completion, Jaap Teunissen for serving as our independent physician, and the scan team: Francisca van der Pluijm, Gertrude Caan, Tiny Cox, and Arlette Almeida. We thank Heleen Voorwinden and Jan de Swart for radiation protection advice, the whole radiolabeling team for their efforts, and the Radiology Trial Office for monitoring. Special thanks are given to Eva Holleman for insights in interpreting pathology data. At the time of submission, Fred Verzijlbergen was employed at Radboud University, Nijmegen, The Netherlands.

KEY POINTS

QUESTION: Is the use of the GRPr antagonist ^{68}Ga-SB3 safe, and is PET/CT imaging of primary PCa sensitive and accurate?

PERTINENT FINDINGS: This clinical trial in a small patient group proceeded without adverse events and showed a sensitivity of 80% for ^{68}Ga-SB3 PET/CT imaging on a patient basis. ^{68}Ga-SB3 has an attractive biodistribution pattern with fast renal clearance and relatively long tumor retention. The 2 PET/CT-negative patients were confirmed to have a GRPr-negative tumor.

IMPLICATIONS FOR PATIENT CARE: ^{68}Ga-SB3 PET/CT is a promising tool for early PCa imaging and, with further research, could aid in staging of primary disease.

REFERENCES

1. Cornelio DB, Roesler R, Schwartsmann G. Gastrin-releasing peptide receptor as a molecular target in experimental anticancer therapy. *Ann Oncol.* 2007;18:1457–1466.
2. Jensen RT, Battey JF, Spindel ER, Benya RV. International Union of Pharmacology. LXVIII. Mammalian bombesin receptors: nomenclature, distribution, pharmacology, signaling, and functions in normal and disease states. *Pharmacol Rev.* 2008;60:1–42.
3. Markwalder R, Reubi JC. Gastrin-releasing peptide receptors in the human prostate: relation to neoplastic transformation. *Cancer Res.* 1999;59:1152–1159.
4. Baratto L, Jadvar H, Iagaru A. Prostate cancer theranostics targeting gastrin-releasing peptide receptors. *Mol Imaging Biol.* 2018;20:501–509.
5. Maina T, Bergsma H, Kulkarni HR, et al. Preclinical and first clinical experience with the gastrin-releasing peptide receptor-antagonist ^{68}Ga-SB3 and PET/CT. *Eur J Nucl Med Mol Imaging.* 2016;43:964–973.
6. Bakker IL, van Tiel ST, Haeck J, et al. In vivo stabilized SB3, an attractive GRPR antagonist, for pre- and intra-operative imaging for prostate cancer. *Mol Imaging Biol.* 2018;20:973–983.
7. Nock B, Nikolopoulou A, Chiotellis E, et al. ^{99m}Tc-demobesin 1, a novel potent bombesin analogue for GRP receptor-targeted tumour imaging. *Eur J Nucl Med Mol Imaging.* 2003;30:247–258.
8. Maina T, Nock BA. From bench to bed: new gastrin-releasing peptide receptor-directed radioligands and their use in prostate cancer. *PET Clin.* 2017;12:205–217.
9. Marsouvanidis PJ, Nock BA, Hajjaj B, et al. Gastrin releasing peptide receptor-directed radioligands based on a bombesin antagonist: synthesis, ^{111}In-labeling, and preclinical profile. *J Med Chem.* 2013;56:2374–2384.
10. Thomas SR, Stabin MG, Chen CT, Samaratunga RC. MIRD pamphlet no. 14 revised: a dynamic urinary bladder model for radiation dose calculations. Task Group of the MIRD Committee, Society of Nuclear Medicine. *J Nucl Med.* 1999;40(suppl):102S–123S.
11. Forrer F, Krenning EP, Kooij PP, et al. Bone marrow dosimetry in peptide receptor radionuclide therapy with ^{177}Lu-DOTA^{0},Tyr^{3}-octreotate. *Eur J Nucl Med Mol Imaging.* 2009;36:1138–1146.
12. Kim MH, Kim HS, Rim KS, et al. The studies on the gastrin levels in the patients with renal failure. *Korean J Intern Med.* 1986;1:43–47.
13. Cimadamore A, Cheng M, Santoni M, et al. New prostate cancer targets for diagnosis, imaging, and therapy: focus on prostate-specific membrane antigen. *Front Oncol.* 2018;8:653.
14. Afshar-Oromieh A, Avtzi E, Giesel FL, et al. The diagnostic value of PET/CT imaging with the ^{68}Ga-labelled PSMA ligand HBED-CC in the diagnosis of recurrent prostate cancer. *Eur J Nucl Med Mol Imaging.* 2015;42:197–209.
15. Dorff TB, Fanti S, Farolfi A, Reiter RE, Sadun TY, Sartor O. The evolving role of prostate-specific membrane antigen-based diagnostics and therapeutics in prostate cancer. *Am Soc Clin Oncol Educ Book.* 2019;39:321–330.
16. Roivainen A, Kahkonen E, Luoto P, et al. Plasma pharmacokinetics, whole-body distribution, metabolism, and radiation dosimetry of ^{68}Ga bombesin antagonist BAY 86-7548 in healthy men. *J Nucl Med.* 2013;54:867–872.
17. Nock BA, Kaloudi A, Lymperis E, et al. Theranostic perspectives in prostate cancer with the gastrin-releasing peptide receptor antagonist NeoBOMB1: preclinical and first clinical results. *J Nucl Med.* 2017;58:75–80.
18. Gnesin S, Cicone F, Mitsakis P, et al. First in-human radiation dosimetry of the gastrin-releasing peptide (GRP) receptor antagonist ^{68}Ga-NODAGA-MJ9. *EJNMMI Res.* 2018;8:108.
19. Minamimoto R, Hancock S, Schneider B, et al. Pilot comparison of ^{68}Ga-RM2 PET and ^{68}Ga-PSMA-11 PET in patients with biochemically recurrent prostate cancer. *J Nucl Med.* 2016;57:557–562.
20. Sun B, Halmos G, Schally AV, Wang X, Martinez M. Presence of receptors for bombesin/gastrin-releasing peptide and mRNA for three receptor subtypes in human prostate cancers. *Prostate.* 2000;42:295–303.
21. Touijer KA, Michaud L, Alvarez HAV, et al. Prospective study of the radiolabeled GRPR antagonist BAY86-7548 for positron emission tomography/computed tomography imaging of newly diagnosed prostate cancer. *Eur Urol Oncol.* 2019;2:166–173.
22. Baum RP, Prasad V, Frischknecht M, Maecke HR, Reubi JC. Bombesin receptor imaging in various tumors: First results of Ga-68 AMBA PET/CT [abstract]. *Eur J Nucl Med Mol Imaging.* 2007;34(suppl 2):S193.
23. Thomas R, Chen J, Roudier MM, Vessella RL, Lantry LE, Nunn AD. In vitro binding evaluation of ^{177}Lu-AMBA, a novel ^{177}Lu-labeled GRP-R agonist for systemic radiotherapy in human tissues. *Clin Exp Metastasis.* 2009;26:105–119.
24. Artinyan A, Soriano PA, Prendergast C, Low T, Ellenhorn JD, Kim J. The anatomic location of pancreatic cancer is a prognostic factor for survival. *HPB (Oxford).* 2008; 10:371–376.
25. Bakker IL, Konijnenberg M, Maina T, et al. From mouse to man: translational properties of $^{67/68}$Ga-sarabesin 3, a GRP-r antagonist, in mouse models versus primary prostate cancer patients [abstract]. *J Nucl Med.* 2016;57(suppl 2):584–584.
26. Lymperis E, Kaloudi A, Sallegger W, et al. Radiometal-dependent biological profile of the radiolabeled gastrin-releasing peptide receptor antagonist SB3 in cancer theranostics: metabolic and biodistribution patterns defined by neprilysin. *Bioconjug Chem.* 2018;29:1774–1784.